

“Research Note”

ACCURATE ANALYSIS AND DESIGN OF CIRCULARLY POLARIZED DUAL-FEED MICROSTRIP ARRAY ANTENNA USING MULTI-PORT NETWORK MODEL*

A. HABIBZADEH-SHARIF^{1,2**}, A. H. YAMINI^{2,3}, AND M. SOLEIMANI²

¹Iran Telecommunication Research Center (ITRC), Tehran, I. R. of Iran

²Iran University of Science & Technology (IUST), Tehran, I. R. of Iran

³Concordia University, Montreal, Quebec, H3G 1M8, Canada

E-Mail: sharif@iust.ac.ir

Abstract– Microstrip Patch Antennas (MPAs) with circular polarization are used in many communication and radar systems. There are several methods and models to analyze and design these antennas. The Multiport Network Model (MNM) is considered one of the best models for MPAs. This model includes several interconnected circuit networks, each of which represents one characteristic of the MPA. The solution of this model is equivalent to the calculation of the input and radiation parameters of the antenna. In this paper, a circularly polarized 2×2 array antenna with sequentially rotated microstrip elements is designed using MNM. In order to produce the circular polarization, besides the sequentially rotation technique, two probe feeds are used in the E-plane and H-plane of each element. These probes are fed by current sources with equal amplitudes and a 90 degree phase difference.

Keywords–Circular polarization, dual-feed, microstrip patch antenna, multiport network model

1. INTRODUCTION

Nowadays, circularly polarized MPAs are one type of conventional antennas in communication and radar systems. The most important characteristics of these antennas are:

- Competition to faraday rotation
- Reduction of the raindrops reflection effects
- No need to estimate the necessary orientation of the antenna according to the polarization of the received signals
- Duplicating the channel capacity using the positive and negative circular polarization
- Reduction of the fading effects

MNM is one of the best models for MPAs analysis and design [1, 2]. This model, in fact, is an extension of the well-known Cavity Model. In the MNM, the underneath and external fields of the patch are separately modeled. The patch is modeled with a multiport 2-D planar network. Mutual coupling effects are considered by the mutual coupling network [3]. The final model includes several circuit networks connected to each other. Input impedance and the voltage of the antenna edge-ports are achieved directly by solving the final model. The other input and radiation parameters of the antenna are achieved from input impedance and edge-ports voltage, respectively [1, 2].

*Received by the editors November 30, 2005; final revised form January 22, 2007.

**Corresponding author

2. DESIGN OF DUAL-FEED CIRCULARLY POLARIZED MPA

Rectangular MPAs are intrinsically linearly polarized antennas. One of the best techniques to create a circularly polarized wave using these antennas is the excitation of two perpendicular modes with equal amplitudes and a 90 degree phase difference, using two probe feeds, respectively in the E-plane and H-plane. These probes have currents with equal amplitudes, but a 90 degree phase difference (Fig. 1). The patch structure and its simple MNM are shown in Figs. 2 and 3, respectively.

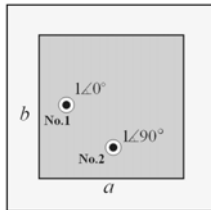


Fig. 1. Circularly polarized dual-feed patch

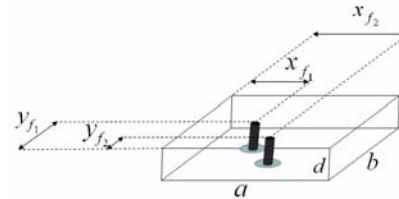


Fig. 2. Structure of dual-feed patch

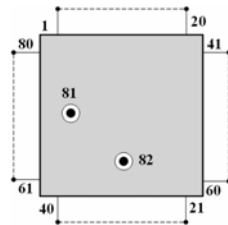


Fig. 3. Simple MNM of dual-feed patch

In this design, 82 ports are considered in the MNM of the dual-feed patch. The patch dimensions and dielectric material are designed for a resonance frequency of 2.45 GHz (Table 1).

Table 1. Antenna specifications

Square patch	$a = 4 \text{ cm}$	$b = 4 \text{ cm}$
$d = 0.079375 \text{ cm}$	$\epsilon_r = 2.33$	$\tan \delta = 0.0012$
$x_{f_1} = ?$	$y_{f_1} = b/2$	$x_{f_2} = a/2$
		$y_{f_2} = ?$

a) Determination of feed location

In this design x_{f_1} and y_{f_2} are determined to achieve the 50Ω input impedance in both ports. Accurate values for x_{f_1} and y_{f_2} are obtained using the input resistance curve versus the feed port location. This curve for both ports is shown in Fig. 4. From this figure it is shown that $x_{f_1} = 1.21 \text{ cm}$ and $y_{f_2} = 1.21 \text{ cm}$, satisfying the antenna impedance matching. Clearly x_{f_1} and y_{f_2} are equal, because the patch structure is square and the feeds are in diagonal symmetry.

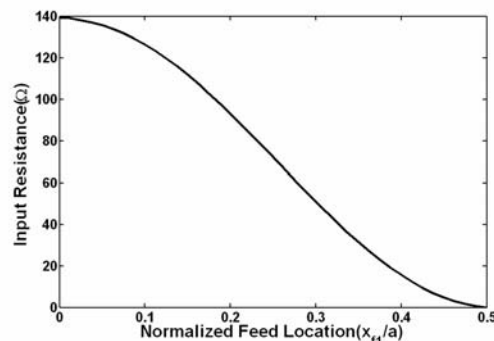


Fig. 4. Input resistance of the patch at ports #81 and #82

b) Simulation results

Simulation results based on MNM are shown in Figs. 5-11.

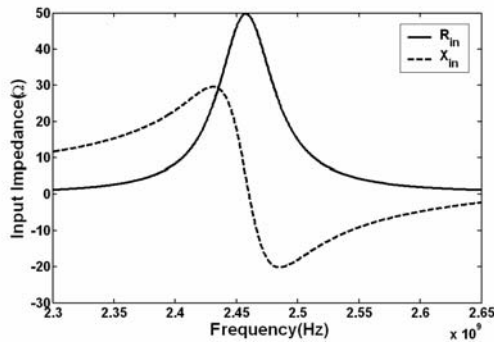


Fig. 5. Input impedance in both ports

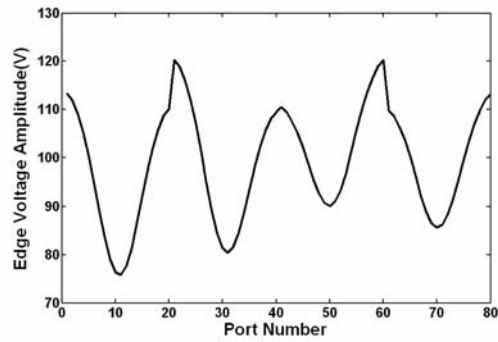


Fig. 6. Amplitude of edge-ports voltage

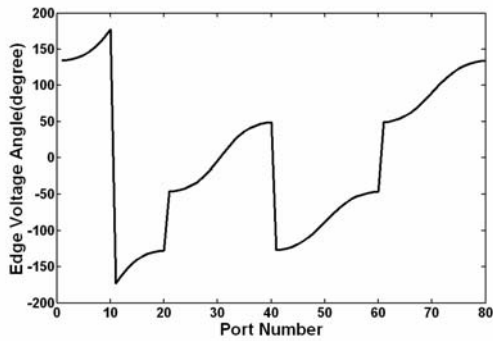


Fig. 7. Angle of edge-ports voltage

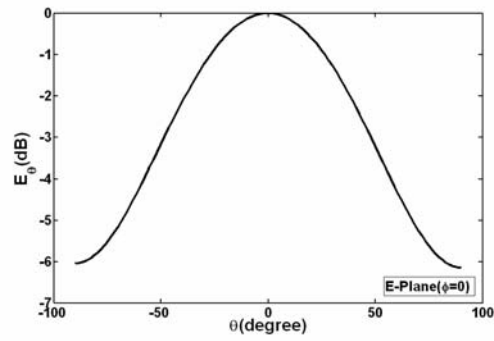


Fig. 8. E-plane radiation pattern of E_0

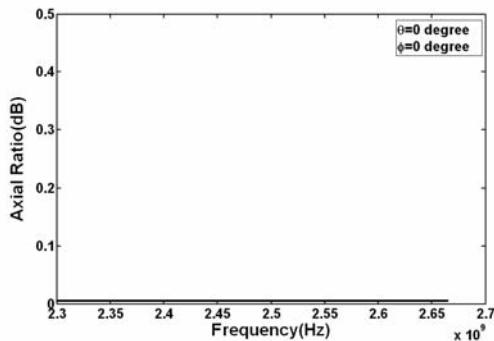


Fig. 9. Axial ratio of total radiation pattern

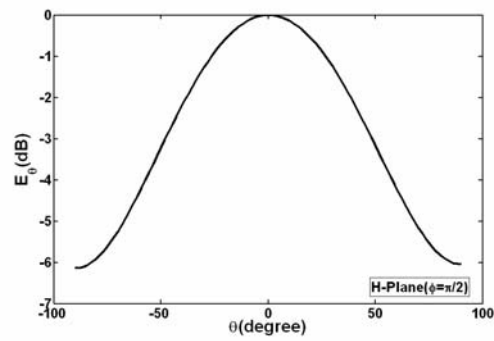


Fig. 10. H-plane radiation pattern of E_0

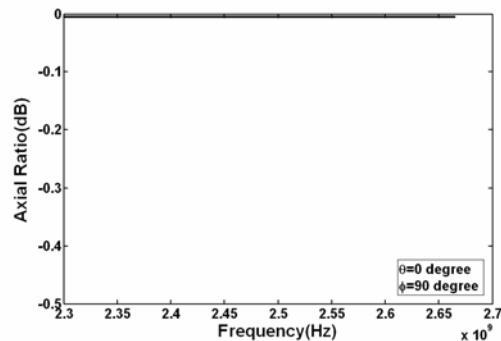


Fig. 11. Axial ratio of the total radiation pattern

c) Discussion

As shown in Fig. 5, the designed antenna has very good impedance matching at 2.46 GHz. Figures 6 and 7 show the amplitude and angle of the edge-ports voltage, respectively. Finally, Figs. 8 and 10 show the conventional radiation patterns. The axial ratio of 0 dB in the frequency range of 2.3-2.7 GHz is shown in Figs. 9 and 11 for different angles of θ and ϕ .

In a multiport network model, magnetic currents on the edges of the patch are calculated from [1]

$$\vec{M} = 2(\vec{E} \times \hat{n}) \quad (1)$$

where, \vec{E} is the electric field at the edge of the patch, and \hat{n} is the unit vector perpendicular to the edge of the patch (in parallel to the antenna surface).

Figure 12 depicts the graphical model of the magnetic currents on the edge of the patch. In this figure, M indicates the magnitude of the magnetic current vector \vec{M} .

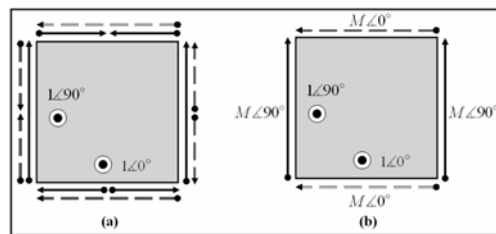


Fig. 12. Graphical model of magnetic currents of the patch

The solid and dashed line magnetic currents in this figure are due to $1\angle 90^\circ$ and $1\angle 0^\circ$ feed ports, respectively. Three different currents are identified on each edge, two of which are in opposite directions. Consequently, the third current can be assumed as the dominant current.

The patch antenna is considered as a linear structure and superposition can be applied to the dual-feed antenna shown in Fig. 1. As a result, it is possible to consider two distinct single-feed patch antennas in simulations instead of a dual-feed one. On the other hand, single-feed patch antennas are linearly polarized. The orthogonality between two dominant out-of-phase magnetic currents shown in Fig. 12b, leads to orthogonal electric far-fields, produced independently by each of the feeds. A 90° phase difference between these two fields provides a circularly polarized wave.

As an example, for the dual-feed patch antenna shown in Fig. 12b, the magnetic currents $M\angle 0^\circ$ and $M\angle 90^\circ$ produce $E_\theta\angle 0^\circ$ and $E_\theta\angle 90^\circ$ radiation fields, respectively. The result of the linear combination of these fields is a circular polarized electrical field. Then, using this feeding structure, a very good circular polarization is achieved.

3. DESIGN OF THE SEQUENTIALLY ROTATED ARRAY

The array structure and its MNM are shown in Figs. 13 and 14, respectively.

Array elements are dual-feed patches designed in section 2 (Fig. 1). The operating frequency is an ISM band of 2.45 GHz. As discussed earlier, these patches produce circularly polarized waves due to a 90° degree phase difference between their perpendicular feeds. As a consequence, the array has a circular polarization.

The specifications of the designed array are summarized in Table 2. The appropriate feed locations are chosen so that impedance matching at all input ports is achieved. Suppose S as the center to center distance between adjacent patches. This distance should be smaller than $0.5\lambda_0$ to prevent the production of grating lobes in the array pattern [4].

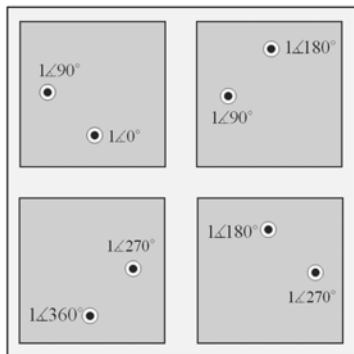


Fig. 13. Circularly polarized 2×2 array

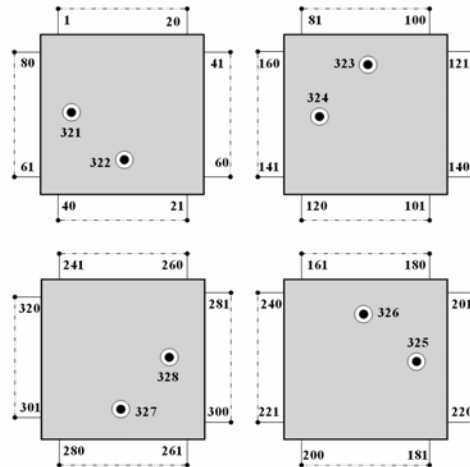


Fig. 14. MNM of the circularly polarized 2×2 array

Table 2. Array specifications

$a = 4 \text{ cm}$		$b = 4 \text{ cm}$	$S = 0.47\lambda_0$
$d = 0.079375 \text{ cm}$		$\epsilon_r = 2.33$	$\tan \delta = 0.0012$
$x_{f_1} = 1.21 \text{ cm}$	$y_{f_1} = b/2$	$x_{f_2} = a/2$	$y_{f_2} = 1.21 \text{ cm}$

a) Calculation of the input impedance of the probe fed patch antenna

If the input parameters of each element are seen from the connecting point of the coaxial cable to the connector, the resistive and inductive effects of the probe length inside the substrate should be taken into account. In the cavity model as the base of MNM, a perfect magnetic wall is considered around the patch. In this case, very complicated equations should be solved to find the probe resistance and inductance. However, if the probe radius is very small, the stored magnetic energy will concentrate more on the probe surroundings. Therefore, with a good approximation we can eliminate the cavity magnetic walls and assume an infinite dimension for the upper and lower planes of the cavity. Then we have an infinite parallel plane waveguide with a wire current between the upper and lower planes [5]. According to the above assumption, the probe impedance is calculated from the following formulas [6]:

$$Z_{probe} = R_{probe} + jX_{probe} \tag{2}$$

$$R_{probe} = \frac{\omega\mu_0 d}{4} \tag{3}$$

$$X_{probe} = \frac{\eta_0}{2\pi} k_0 d \left\{ -\gamma + \ln \left(\frac{2}{\sqrt{\epsilon_r} k_0 r} \right) \right\} \tag{4}$$

where ω , η_0 , k_0 , μ_0 , r and d are angular frequency, free space characteristic impedance, phase constant, free space permeability, probe radius and substrate thickness, respectively. Also, γ is the Euler number which is equal to 0.5772156649.

According to Eqs. (3) and (4), both resistance and inductive reactance are increased by increasing the substrate thickness. Considering the probe impedance, the circuit model shown in Fig. 15 applies to the patch antenna at frequencies near resonance [5]. In this figure the patch has been modeled as a parallel RLC circuit. The input impedance of the patch is:

$$Z_{in_{patch}} = R || L || C \tag{5}$$

The input impedance of the probe fed patch antenna is obtained from:

$$Z_{in_{eq}} = Z_{probe} + Z_{in_{patch}} \tag{6}$$

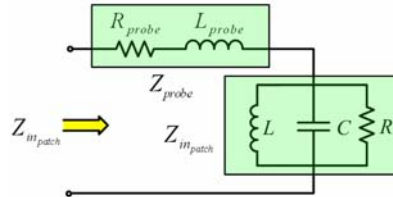


Fig. 15. CAD model for the probe fed patch antenna

b) Simulation results

Some of the simulation results of the array based on MNM are shown in Figs. 16 to 21.

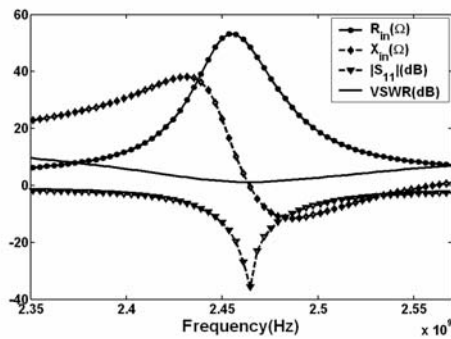


Fig. 16. Input parameters in port #321

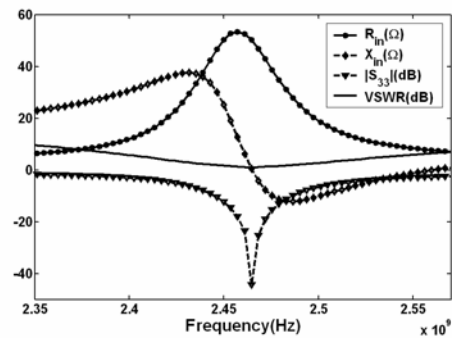


Fig. 17. Input parameters in port #323

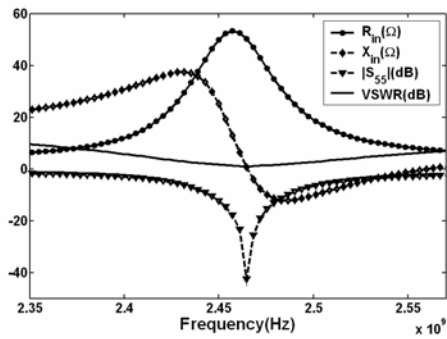


Fig. 18. Input parameters in port #325

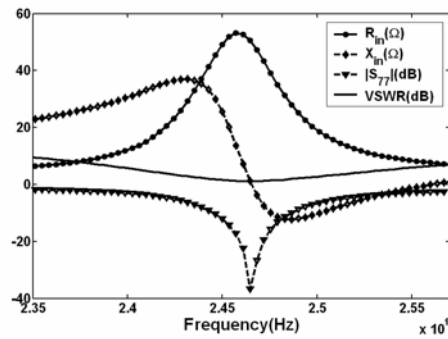


Fig. 19. Input parameters in port #327

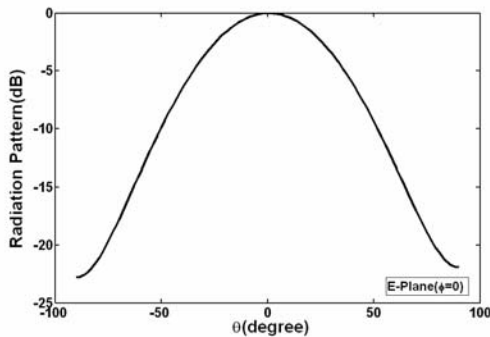


Fig. 20. Radiation pattern of the array

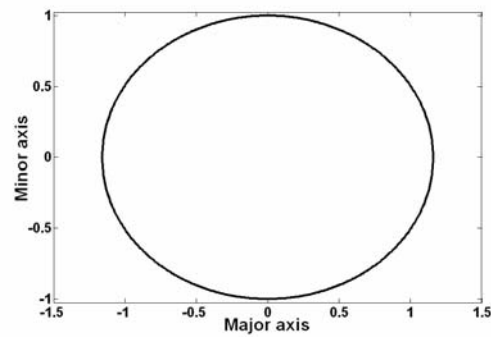


Fig. 21. Polarization ellipse of total radiation pattern for $\theta = 0, \phi = 0$

c) Discussion

As shown in Figs. 16 to 19, impedance matching is achieved in all ports at a frequency near to 2.46 GHz with $S_{ii} < -30$ dB for $i = 1, 2, \dots, 8$. Moreover, Figs. 20 and 21 show the radiation pattern of the array in the E-plane and polarization ellipse of the total radiation pattern for $\theta=0$, and $\phi=0$ at 2.46 GHz. Circular polarization is achieved with a good quality. Figure 22 shows the magnetic current on the edges of the patches. These currents are associated with TM_{10} and TM_{01} modes. In this figure, the current produced by ports #321, #323, #325 and #327 is shown by a dash line, and the current corresponding to ports #322, #324, #326 and #328 is shown by a solid line.

Similar to section 2c, we can consider only a dominant current on each edge (Fig. 23). The phases of magnetic currents are 0° , 90° , 180° , 270° , and 360° in this figure. The phase of 180° corresponds to the current direction in reverse. Therefore, it is possible to replace the magnetic currents with 180° and 270° phases with magnetic currents of opposite directions and 0° and 90° phases, respectively (Fig. 24).

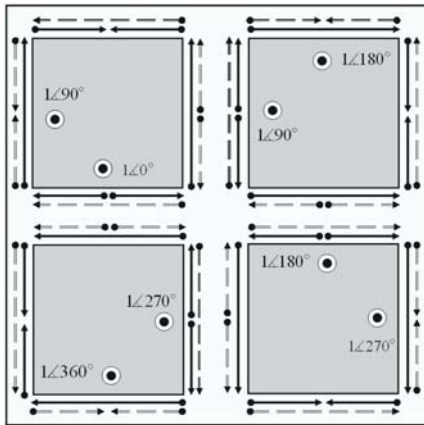


Fig. 22. Magnetic currents in the edges of patches

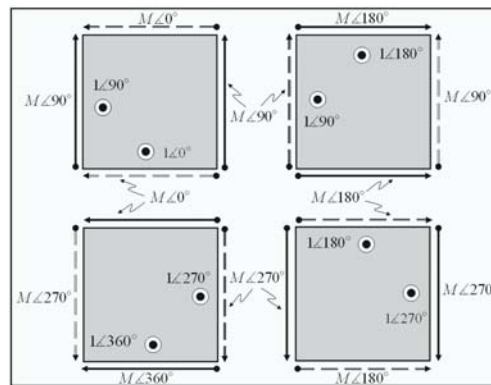


Fig. 23. Dominant magnetic currents

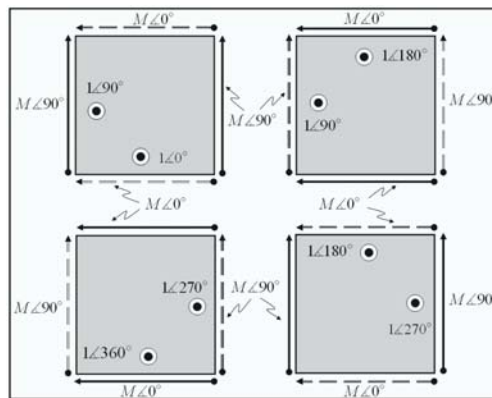


Fig. 24. Equivalent dominant magnetic currents

Magnetic currents $M\angle 0^\circ$ and $M\angle 90^\circ$ generate electrical fields $E_\theta\angle 0^\circ$ and $E_\theta\angle 90^\circ$ respectively. A linear combination of these fields leads to a circularly polarized wave. As a result, these magnetic currents fulfill the production of the circular polarization.

Indeed, the circular polarization observed in the simulation results is confirmed qualitatively.

4. SUMMARY

This paper has indicated the capabilities of the MNM in the analysis and design of useful practical MPAs and its flexibility to model complicated structures. A dual-feed microstrip patch antenna is designed using this technique. The designed antenna is used as an element to develop a 2×2 microstrip array. Obviously, larger radiation gain is achieved in the array antenna compared to that of the single element. One of the most important results of this paper is the fact that, in spite of this exceeding gain, circular polarization has less polarization purity in the array due to a greater distance between in-phase magnetic currents. Investigating the results, new and deep insights into the operation of MPAs are achieved.

REFERENCES

1. Kumar, G. & Ray, K. P. (2003). *Broadband microstrip antennas*. Artech House.
2. James, J. R. & Hall, P. S. (1989). *Handbook of microstrip antennas*. London: Peter Peregrinus Ltd.
3. Benalla, A. & Gupta, K. C. (1989). Multiport network approach for modeling the mutual coupling effects in microstrip patch antennas and arrays. *IEEE Transaction on Antennas and Propagation*, 37(2).
4. Stutzman, W. L. & Thiele, G. A. (1997). *Antenna theory and design*. Wiley Text Books.
5. Lee, K. F. & Chen, W. (1997). *Advances in microstrip and printed antennas*. John Wiley & Sons.
6. Damiano, J. P. & Papiernik, A. (1994). Survey of analytical and numerical models for probe-fed microstrip antennas. *IEE Proc., Microw. Antennas Propag.*, 141(1).